

# Tunneling Anisotropic Magnetoresistance and Spin-Orbit Coupling in Fe/GaAs/Au Tunnel Junctions

J. Moser,\* A. Matos-Abiague, D. Schuh, W. Wegscheider, J. Fabian, and D. Weiss

*Institut für Experimentelle und Angewandte Physik,  
Universität Regensburg, 93040 Regensburg, Germany*

(Dated: October 31, 2018)

We report the observation of tunneling anisotropic magnetoresistance effect (TAMR) in the epitaxial metal-semiconductor system Fe/GaAs/Au. The observed two-fold anisotropy of the resistance can be switched by reversing the bias voltage, suggesting that the effect originates from the interference of the spin-orbit coupling at the interfaces. Corresponding model calculations reproduce the experimental findings very well.

PACS numbers: 73.43.Jn, 72.25.Dc, 73.43.Qt

Tunneling magnetoresistance (TMR) devices consist of a tunneling barrier, typically an oxide, sandwiched between two ferromagnetic layers of different coercive fields. Such systems find widespread use in sensor and memory application as they exhibit a large resistance difference for parallel and antiparallel alignment of the ferromagnets' magnetization [1]. The TMR effect relies, within the simplest model [2], on the different spin polarizations at the Fermi energy  $E_F$  in the ferromagnets; it is absent if one ferromagnetic layer is replaced by a normal metal. Hence it came as a surprise that a spin-valve-like tunnel magnetoresistance was found in (Ga,Mn)As/alumina/Au sandwiches [3]. The origin of the effect, labeled tunneling anisotropic magnetoresistance (TAMR), was associated with the anisotropic density of states in the ferromagnet (Ga,Mn)As. An enhanced anisotropic magnetoresistance (AMR) effect measured across a constriction in a (Ga,Mn)As film was ascribed to the TAMR effect, too [4]. In both experiments the fourfold symmetry, expected if the (Ga,Mn)As hole density of states is involved, was broken and ascribed to strain in (Ga,Mn)As.

Here we show that a TAMR effect can also be observed in sandwiches involving a conventional ferromagnet like iron. A stack of Fe, GaAs and Au, with iron grown epitaxially on the GaAs tunneling barrier, shows pronounced spin-valve-like signatures. We observe a uniaxial anisotropy of the tunneling magnetoresistance. Depending on the bias voltage the high resistance state is either observed for the magnetization  $\mathbf{M}$  oriented in [110] or in [1̄10] direction. We propose a theoretical model in which the  $C_{2v}$  symmetry, resulting from the interference of Bychkov-Rashba and Dresselhaus spin-orbit interactions, is transferred to the tunneling probability, giving rise to the observed two-fold symmetry.

A sketch of the system is shown in Fig. 1(a). The 13 nm thick epitaxial iron layer was grown on an 8 nm thin GaAs (001) barrier by transferring the freshly grown GaAs heterojunction from the molecular beam epitaxy chamber to a magnetron sputtering system without breaking the ultrahigh vacuum (UHV). The quality of the interface of a sample from the same wafer was checked

by high-resolution transmission electron microscopy [5]. The Fe layer was covered by 50 nm cobalt and 100 nm gold which serves as back contact. The wafer then was glued upside down to another substrate and the original substrate was etched away. Finally, the circular, 150 nm thick top gold contact was made by employing optical lithography, selective etching of AlGaAs, and UHV magnetron sputtering. At the Fe/GaAs and the Au/GaAs interfaces Schottky barriers form. The barrier heights can depend on the preparation techniques [6] and were assumed to be 0.75 eV on each side, which was found for the Fe/GaAs interface [7]. Hence the GaAs layer constitutes a nearly rectangular barrier allowing, e.g., observation of the TMR [5, 7]. In total, four batches of samples which differ in the preparation of the Au layer (with and without  $H^+$ -plasma etching step, see e.g. Ref. [5]) or in an additional annealing step (150° Celsius for 1 hour) were investigated. As the described features are essentially independent of these details we focus on the results of one sample (annealed without  $H^+$ -plasma etching) below.

The measurements were carried out at 4.2 K using a variable temperature insert of a  $^4\text{He}$ -cryostat with a superconducting coil to generate the external magnetic field  $\mathbf{B}$ . We used a Semiconductor Analyzer HP 4155A to probe the resistance drop across the GaAs barrier in four-point configuration. Therefore the top Au contact was grounded. To vary the direction  $\mathbf{M}$  of iron, the sample was mounted in a rotatable sample holder enabling a 360° in-plane rotation of  $\mathbf{B}$ . The direction of  $\mathbf{B}$  is given by its angle with respect to the hard [110] direction (nomenclature with respect to GaAs crystallographic directions). The I-V-characteristics, measured between top gold and bottom Fe contact, is strongly nonlinear (not shown). This suggests that electron transport through the barrier is, as in previous TMR experiments, dominated by quantum mechanical tunneling [7].

Our Letter is about the anisotropy of the tunneling resistance with respect to the in-plane magnetization  $\mathbf{M}$  of the iron contact. Epitaxial iron has both a cubic anisotropy of bulk iron as well as an uniaxial contribution stemming from the interface. Magnetization reversal for

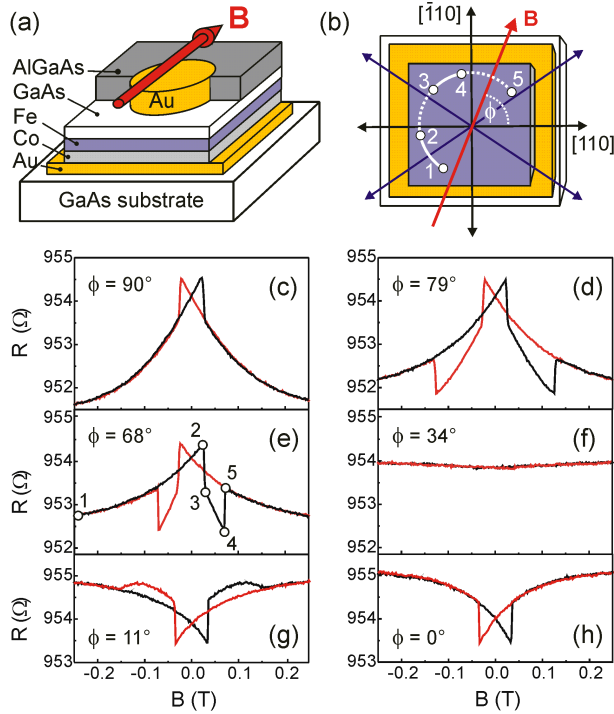


FIG. 1: (a) Schematic picture of a Fe/GaAs/Au tunnel structure; (b) schematic top view on the iron layer; (c)-(h) tunneling resistance depending on the magnetic field  $\mathbf{B}$  swept under different angles  $\phi$  measured at 4.2 K and -90 mV bias (Au contact grounded). The double step switching mechanism is illustrated in (b) and (e) (see text).

an in-plane magnetic field typically takes place in two steps explained by nucleation and propagation of  $90^\circ$  domain walls [8]. Figs. 1(c) - 1(h) display the tunneling resistance as a function of magnetic field  $\mathbf{B}$  swept in different in-plane directions at a bias voltage of -90 mV and a temperature of  $T = 4.2$  K. Fig. 1(c) shows the resistance for the magnetic field swept at an angle of  $\phi = 90^\circ$  ([T10] direction) from negative saturation to positive saturation and back. The figure focuses on the interesting region between -0.25 T and +0.25 T. A clear spin-valve like signal characterized by one switching event (one jump in  $R$ ) is observed for the resistance if  $\mathbf{B}$  is applied along this hard direction. If  $\mathbf{B}$  is applied  $11^\circ$  off the hard [T10] axis the characteristic second switching process occurs at  $\sim 0.12$  T, as is manifested in Fig. 1(d). Decreasing  $\phi$  the second switching point is shifted towards smaller  $B$  [Fig. 1(e)]. This two step switching process is described in more detail for  $\phi = 68^\circ$  in Fig. 1(e). Starting close to saturation at  $-\mathbf{B}$  [point 1 in Fig. 1(b)], the average magnetization direction moves towards the hard magnetic [T10]-axis (point 2) if  $\mathbf{B}$  is reversed and increased towards positive field values. In the first step  $\mathbf{M}$  switches from near the easy axis closest to the original direction of  $\mathbf{B}$  beyond the easy axis located  $90^\circ$  sideways from this one (point 3). Increasing  $\mathbf{B}$  further drives  $\mathbf{M}$  towards

the [T10] direction (point 4) until, in the second switching event,  $\mathbf{M}$  jumps near the easy direction closest to the new  $\mathbf{B}$ -direction (point 5). The signal disappears if  $\mathbf{B}$  is swept along an easy direction - in the present sample lying at  $\phi = 34^\circ$  - [Fig. 1(f)] and changes sign for  $\mathbf{B}$  close to [Fig. 1(g)] or along the hard [110] direction [Fig. 1(h)].

Though reminiscent of the AMR effect the results presented here cannot be explained by the conventional AMR effect of the iron layer. The resistance change caused by the AMR effect of the iron layer of only about 4 m $\Omega$  is much smaller than the the observed change in the tunneling resistance of about 3.5  $\Omega$ . So the AMR effect can be excluded as physical origin of the measurement and the question for the origin of the anisotropic resistance remains.

The symmetry of the anisotropic tunneling magnetoresistance becomes more explicit at higher  $\mathbf{B}$  where  $\mathbf{M}$  is forced to follow the direction of the externally applied magnetic field. The data displayed in a polar plot in Fig. 2(a), normalized to the resistance in [110] direction, were taken at  $B = 0.5$  T at a bias voltage of -90 mV and  $T = 4.2$  K. An uniaxial anisotropy evincing the shape of a “horizontal 8” is clearly manifested. The resistance in [T10] direction is typically  $\sim 0.4\%$  smaller than in [110] direction. This anisotropy of the resistance explains the resistance jumps observed in Figs. 1(c)-1(h): The actual position of the (average) magnetization determines the resistance. The direction highlighted by triangles in Fig. 2(a) correspond to the directions, taken up by the magnetization  $\mathbf{M}$  in Fig. 1(e) for the marked  $\mathbf{B}$  values. The thin red line is the result of a model calculation with one adjustable parameter as pointed out below.

The anisotropy depends on the applied bias voltage. If the bias voltage is reversed from -90 mV to +90 mV the “8” is rotated by  $90^\circ$  as shown in Fig. 2(b). The bias dependencies of the resistances’ angular characteristics is summarized in Fig. 2(c). While for bias voltages  $V > 50$  mV the resistance is larger for the [T10] directions, for  $V < 50$  mV the resistances are largest for the [110] directions. Similar behavior was found for all samples investigated.

We now introduce a model ascribing the observed anisotropy to anisotropic spin orbit interaction. It has already been stated in reference to GaMnAs junctions [3, 9, 10, 11] that the effect is due to spin-orbit coupling. However, to capture the  $C_{2v}$  symmetry of the observed TAMR, a uniaxial strain has been invoked [3] lowering the four-fold symmetry of the GaMnAs density of states. On the other hand, ab-initio calculations in CoPt [11] suggest that strain is not necessary to have anisotropic electronic structure in layered systems. What then leads to the twofold symmetry of the TAMR? We argue here that TAMR in epitaxial systems does not need an *ad hoc* anisotropic density of states. Instead, the tunneling probability itself is strongly anisotropic due to the interfacial spin-orbit coupling. We propose that the two-fold sym-

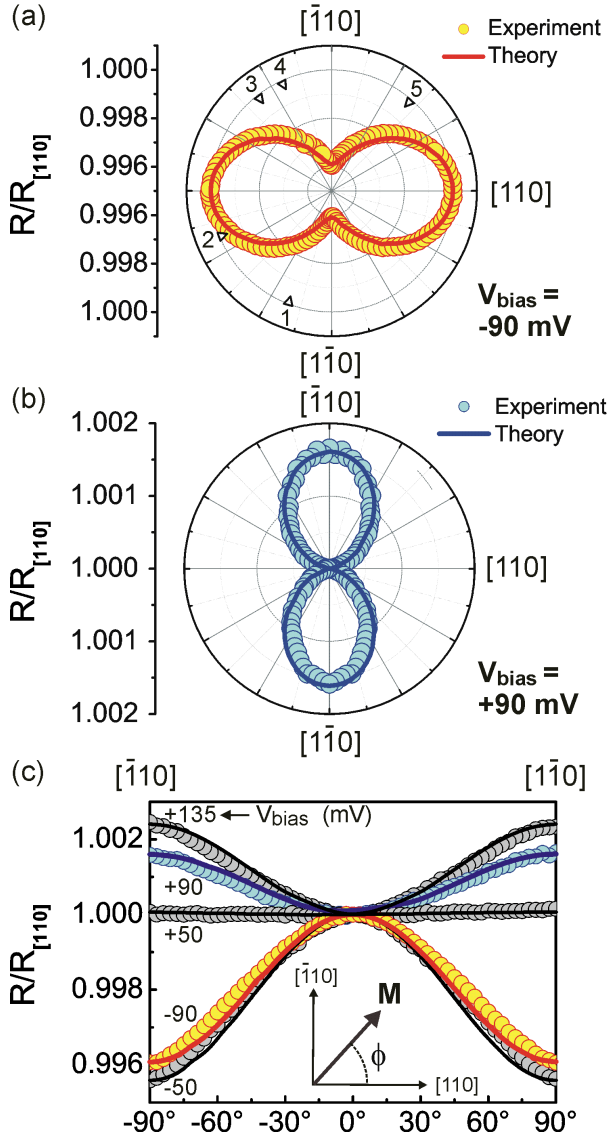


FIG. 2: a)  $\phi$ -scan of the tunneling resistance at 4.2 K and -90 mV bias in a saturation magnetic field  $|\mathbf{B}| = 0.5$  T and  $|\mathbf{B}| = 10$  T and a theoretical fit; b)  $\phi$ -scan at +90 mV; c)  $\phi$ -scans for different bias voltages. Symbols correspond to experimental results for -90 mV, -50 mV, 50 mV, 90 mV and 135 mV bias; solid lines correspond to theoretical results with  $\alpha_l = 42.3 \text{ eV } \text{\AA}^2$ ,  $\alpha_l = 45.8 \text{ eV } \text{\AA}^2$ ,  $\alpha_l = -0.6 \text{ eV } \text{\AA}^2$ ,  $\alpha_l = -17.4 \text{ eV } \text{\AA}^2$ ,  $\alpha_l = -25.1 \text{ eV } \text{\AA}^2$  respectively.

metry of the TAMR is a consequence of the anisotropic spin-orbit interaction (SOI) that reflects the bulk and structure inversion asymmetries of our system. Indeed, the combination of bulk inversion asymmetry (Dresselhaus SOI) [12, 13, 14] and structure inversion asymmetry (Bychkov-Rashba SOI) [14] in GaAs-like semiconductor heterostructures leads to a spin-orbit interaction with  $C_{2v}$  symmetry. Based on this observation we consider the following model Hamiltonian for describing the tun-

nelling across our metal/semiconductor heterojunction:

$$H = H_0 + H_Z + H_{BR} + H_D. \quad (1)$$

Here

$$H_0 = -\frac{\hbar^2}{2} \nabla \left[ \frac{1}{m(z)} \nabla \right] + V_z, \quad (2)$$

with  $m(z)$  the electron effective mass [in terms of the bare electron mass  $m_0$  we assume  $m = m_c = 0.067 m_0$  in the central (GaAs) region and  $m = m_l = m_r \approx m_0$  in the left (Fe) and right (Au) regions] and  $V(z)$  the conduction band profile defining the potential barrier along the growth direction ( $z$ ) of the heterostructure [see Fig. 3(a)].

The Zeeman spin splitting due to the exchange field (in the Fe region) and the external magnetic field in the Fe and Au (the Zeeman energy in GaAs is much smaller than all the other energy scales characterizing the system and we can therefore neglect its effect) is given by

$$H_Z = -\frac{\Delta(z)}{2} \mathbf{n} \cdot \boldsymbol{\sigma}. \quad (3)$$

Here  $\Delta(z)$  represents the Zeeman energy in the different regions,  $\boldsymbol{\sigma}$  is a vector whose components are the Pauli matrices, and  $\mathbf{n}$  is a unit vector defining the spin quantization axis determined by the in-plane magnetization direction in Fe.

The Bychkov-Rashba SOI due to the structure inversion asymmetry at the interfaces can be written as [15]

$$H_{BR} = \frac{1}{\hbar} \sum_{i=l,r} \alpha_i (\sigma_x p_y - \sigma_y p_x) \delta(z - z_i), \quad (4)$$

where,  $\alpha_l$  ( $\alpha_r$ ) denotes the SOI strength at the left (right) interface  $z_l = 0$  ( $z_r = d$ ). We note that inside the GaAs barrier, away from the interfaces, there is also a Bychkov-Rashba SOI contribution induced by the applied bias. However, this contribution is negligible for our system and we neglect it.

The Dresselhaus SOI resulting from the bulk inversion asymmetry in GaAs is incorporated in the model through the term [13, 14, 16, 17, 18]

$$H_D = \frac{1}{\hbar} (\sigma_x p_x - \sigma_y p_y) \frac{\partial}{\partial z} \left( \gamma(z) \frac{\partial}{\partial z} \right), \quad (5)$$

where the Dresselhaus parameter  $\gamma \approx 24 \text{ eV } \text{\AA}^3$  in the GaAs region [14, 16, 17, 18] and  $\gamma = 0$  elsewhere.

The current flowing along the heterojunction is given by

$$I = \frac{e}{(2\pi)^3 \hbar} \sum_{\sigma=-1,1} \int dE d^2 k_{\parallel} T_{\sigma}(E, \mathbf{k}_{\parallel}) [f_l(E) - f_r(E)], \quad (6)$$

where  $\mathbf{k}_{\parallel}$  is the in-plane wave vector and  $f_l(E)$  and  $f_r(E)$  are the electron Fermi-Dirac distributions with chemical

potentials  $\mu_l$  and  $\mu_r$  in the left and right leads, respectively. The particle transmissivity  $T_\sigma(E, \mathbf{k}_\parallel)$  is found, as usually, after solving for the scattering states in the different regions.

Calculations for the dependence of the resistance on the angle  $\theta$  between the magnetization in Fe and the [100] direction (note that  $\theta = \phi + \pi/4$ ) were carried out at zero temperature and a barrier high (measured from the Fermi energy) of 0.75 eV. For the Fe layer we assume a Stoner model with the majority and minority spin channels having Fermi momenta  $k_{F\uparrow} = 1.05 \times 10^8 \text{ cm}^{-1}$  and  $k_{F\downarrow} = 0.44 \times 10^8 \text{ cm}^{-1}$  [19], respectively. The Fermi momentum in Au was assumed to be  $\kappa_F = 1.2 \times 10^8 \text{ cm}^{-1}$  [20].

The values of the Bychkov-Rashba parameters  $\alpha_l$ ,  $\alpha_r$  [see Eq. (4)] are not known for metal-semiconductor interfaces. Due to the complexity of the problem, a theoretical estimation of such parameters requires first principle calculations including the band structure details of the involved materials, which is beyond the scope of the present paper. Here we assume  $\alpha_l$  and  $\alpha_r$  as phenomenological parameters. We have found that due to the large exchange splitting in the left (Fe) region, the calculated TAMR is dominated by  $\alpha_l$ ; the dependence on  $\alpha_r$  is negligible and we can set  $\alpha_r = 0$ . This leaves only  $\alpha_l$  as a fitting parameter in the comparison of the theoretical and experimental value of the ratio  $R_{[1\bar{1}0]}/R_{[110]}$ . Such a comparison is displayed in Fig. 2(a) for the case of an external bias  $V_0 = -90 \text{ meV}$  and low magnetic field  $B = 0.5 \text{ T}$ . The agreement between theory and experiment is indeed very satisfactory, considering that we fit the value of  $\alpha_l$  (the fit is  $42.3 \text{ eV \AA}^2$ ) only for the direction  $\phi = \pi/2$  — this is enough for our theoretical model to reproduce the *complete* angular dependence of  $R(\phi)/R_{[110]}$ . Preliminary ab-initio calculations confirm qualitatively the above picture [21].

We have performed the same fitting procedure for other values of the applied voltage. The results are shown in Figs. 2(b) and (c), where the good agreement between theory and experiment is apparent. Different values of  $\alpha_l$  are obtained when varying the bias voltage, suggesting that the interface Bychkov-Rashba parameters are voltage dependent (unlike  $\gamma$ , which is a material parameter), as found in other systems [1]. The interface Bychkov-Rashba parameter,  $\alpha_l$ , in our system changes sign at a bias slightly below 50 mV.

The robustness of the fit points to the following phenomenological model of the TAMR. Averaging the SOI  $H_{SOI} = H_{BR} + H_D$  [see Eqs. (4) and (5)] over the states of the system one obtains  $H_{SOI} \sim \mathbf{w}(\mathbf{k}_\parallel) \cdot \boldsymbol{\sigma}$  [17], where  $\mathbf{w}(\mathbf{k}_\parallel) = (\tilde{\alpha}k_y - \tilde{\gamma}k_x, -\tilde{\alpha}k_x + \tilde{\gamma}k_y, 0)$ . Here  $\tilde{\alpha}$  and  $\tilde{\gamma}$  are effective Bychkov-Rashba and Dresselhaus parameters that measures the SOI induced spin precession of the electrons during tunneling. There are only two preferential directions defined by  $\mathbf{n}$  and  $\mathbf{w}(\mathbf{k}_\parallel)$  [see Fig. 3(b)]. Therefore, the anisotropy of a scalar quantity such as the

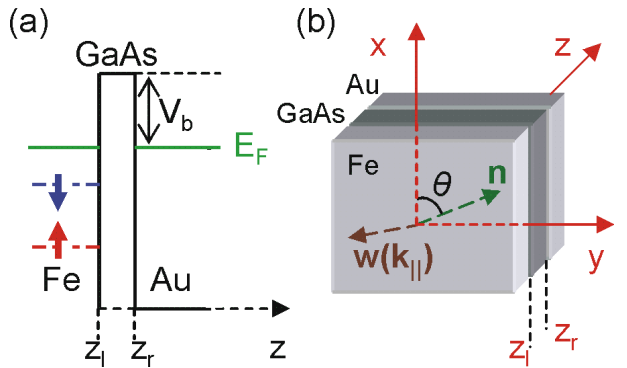


FIG. 3: (a) Schematics of the conduction band profile along the growth direction of the heterostructure. (b) A spacial view of the model system. The vector  $\mathbf{n}$  determines the magnetization direction in Fe with respect to the [100] direction ( $x$  axis). The SOI induced spin precession of the electrons during tunneling is characterized by the vector  $\mathbf{w}(\mathbf{k}_\parallel)$  (see text).

total transmissivity is obtained as a perturbative series of  $\mathbf{n} \cdot \mathbf{w}(\mathbf{k}_\parallel)$ , since the SOI is much smaller than the other relevant energy scales in the system. Averaging over the in-plane momenta to get the full current, the anisotropy is determined, up to the second order, by  $\langle [\mathbf{n} \cdot \mathbf{w}(\mathbf{k}_\parallel)]^2 \rangle$  [the first-order term vanishes, since  $\mathbf{w}(\mathbf{k}_\parallel) = -\mathbf{w}(-\mathbf{k}_\parallel)$ ]. Thus, the tunneling current anisotropy is proportional to  $\tilde{\alpha}\tilde{\gamma} \sin 2\theta$  [22]. Taking into account that  $\theta = \phi + \pi/4$  and that the observed anisotropy is small one obtains for the TAMR,  $R(\phi)/R_{[110]} - 1 \sim \tilde{\alpha}\tilde{\gamma}(\cos 2\phi - 1)$ . This is precisely the kind of angular dependence experimentally found (see Fig. 2). Assuming that the spin-orbit parameters are voltage dependent, one can change the sign and magnitude of the anisotropy,  $\tilde{\alpha}\tilde{\gamma}$ , by varying the bias voltage, as shown in Fig. 2. Notably, if  $\tilde{\alpha}\tilde{\gamma} \approx 0$ , one obtains a suppression of the TAMR effect, a situation corresponding to a bias voltage of 50 mV [Fig. 2(c)].

In summary we observed TAMR in an epitaxial ferromagnet/insulator system and propose that the effect occurs whenever both Rashba and Dresselhaus SOI are involved in the tunneling process.

Financial support by German Science Foundation (DFG) via SFB 689 and by BMBF (nanoQUIT) is gratefully acknowledged.

\* Electronic address: juergen.moser@physik.uni-regensburg.de  
[1] I. Žutić, J. Fabian, and S. Das Sarma, Rev. Mod. Phys.

**76**, 323 (2004).

[2] M. Jullière, Physics Letters **54**, 225 (1975).

[3] C. Gould *et al.*, Phys. Rev. Lett. **93**, 117203 (2004).

[4] A. D. Giddings *et al.*, Phys. Rev. Lett. **94**, 127202 (2005).

[5] J. Moser *et al.*, Appl. Phys. Lett. **89**, 162106 (2006).

[6] Y. G. Wang and S. Ashok, J. Appl. Phys. **75**, 2447 (1994).

- [7] S. Kreuzer *et al.*, *Appl. Phys. Lett.* **80**, 4582 (2002).
- [8] R. P. Cowburn *et al.*, *J. Appl. Phys.* **78**, 7210 (1995).
- [9] C. Rüster *et al.*, *Phys. Rev. Lett.* **94**, 027203 (2005).
- [10] H. Saito, S. Yuasa, and K. Ando, *Phys. Rev. Lett.* **95**, 086604 (2005);
- [11] A. B. Shick, F. Máca, J. Mašek, and T. Jungwirth, *Phys. Rev. B* **73**, 024418 (2006);
- [12] G. Dresselhaus, *Phys. Rev.* **100**, 580 (1955).
- [13] U. Rössler and J. Kainz, *Solid State Commun.* **121**, 313 (2002).
- [14] R. Winkler, *Springer tracts in Modern Physics*, Vol. 191 (Springer, Berlin 2003).
- [15] E. A. de Andrada e Silva, G. C. La Rocca, and F. Bassani, *Phys. Rev. B* **50**, 8523 (1994); *ibid.* **55**, 16293 (1997).
- [16] V. I. Perel *et al.*, *Phys. Rev. B* **67**, 201304(R) (2003).
- [17] S. D. Ganichev *et al.*, *Phys. Rev. Lett.* **92**, 256601 (2004).
- [18] L. G. Wang, W. Yang, K. Chang, and K. S. Chan, *Phys. Rev. B* **72**, 153314 (2005).
- [19] J. Wang, D. Y. Xing, and H. B. Sun, *J. Phys.: Condens. Matter* **15**, 4841 (2003).
- [20] N. W. Ashcroft and N. D. Mermin, *Solid State Physics* (Saunders College, Philadelphia 1988).
- [21] V. Popescu and H. Ebert (private communication).
- [22] A. Matos-Abiague and J. Fabian (unpublished).